

Influence of the concentrations of xanthan gum, hydroxypropyl starch and potassium chloride on the flow properties of drilling fluid formulations

Bruna F. Alves^{1*}, Vera L.C. da Lapa¹, Carla M.F. Silva¹, Elizabete F. Lucas^{2,3}

¹Universidade Estácio de Sá - R. Eduardo Luiz Gomes, 134 - Morro do Estado, Niterói, 24020-340, RJ, Brazil.

²Universidade Federal do Rio de Janeiro, Instituto de Macromoléculas/LMCP – Av. Horácio Macedo, 2030, bloco J, Cidade Universitária, 21941598, RJ, Brazil.

³Universidade Federal do Rio de Janeiro, COPPE, Departamento de Engenharia Metalúrgica e de Materiais/LADPOL, Av. Horácio Macedo, 2030, bloco F, Cidade Universitária, 21941598, RJ, Brazil

Email: *elucas@metalmat.ufrj.br

Abstract

Drilling operation of oil wells involves high costs and risks. With recent discoveries of deeper reservoirs and difficult to access, there was an increase in the number of horizontal wells drilled and far-reaching, and, thereat, new challenges with operational problems. Fluids, or muds, drilling are essential to the well drilling process, confirming the need to study and find physical, rheological, and filtration properties, appropriate to the complexities in each section and the drilling stage. Optimized formulation is the one that comprises a safe operation, mitigation of operational problems, environmental protection, low cost, and high productivity. Thus, this paper offers the study of the rheological properties, and determination of filtrate volume, of the aqueous base fluid formulations, developed with polymeric additives. A high performance formulation, presenting technical-economical feasibility for drilling operations, was achieved using 0.43% m/v of viscosifier (xanthan gum), 0.57% m/v of filtrate controller (hydroxypropyl starch) and 4.57% m/v of clay swelling inhibitor (KCl).

Keywords: drilling fluids, polymeric additives, rheological properties, operational conditions.

Influencia de las concentraciones de goma xantano, hidroxipropil almidón y cloruro de potasio sobre las propiedades de flujo de las formulaciones de fluidos de perforación

Resumen

La operación de perforación de pozos de petróleo implica altos costos y riesgos. Con los recientes descubrimientos de depósitos más profundos y de difícil acceso, hubo un aumento en el número de pozos horizontales perforados y de largo alcance y, por lo tanto, nuevos desafíos con problemas operacionales. Los fluidos o los lodos de perforación son esenciales para el proceso de perforación del pozo, confirmando la necesidad de estudiar y encontrar propiedades físicas, reológicas y de filtración, adecuadas a las complejidades de cada sección ya la fase de perforación. La formulación optimizada es aquella que comprende una operación segura, mitigación de problemas operacionales, protección ambiental, bajo costo y alta productividad. Así, este trabajo ofrece el estudio de las propiedades reológicas y de volumen de filtrado de las formulaciones de fluidos de base acuosa, desarrolladas con aditivos poliméricos. Una formulación de alto rendimiento, presentando viabilidad técnico-económica para operaciones de perforación, fue alcanzada utilizando 0,43% mv de viscosificante (goma xantana), 0,57% m / v de controlador de filtrado (hidroxipropilamido) y 4,57% m / v de inhibidor de la hinchazón de arcilla (KCl).

Palabras clave: fluidos de perforación, aditivos poliméricos, propiedades reológicas, condiciones operativas.

Cita: Alves, B. F., Lapa, V. L. C., Silva F., C. M. & Lucas, E. F. (2019). Influence of the concentrations of xanthan gum, hydroxypropyl starch and potassium chloride on the flow properties of drilling fluid formulations. *Revista Fuentes: El reventón energético*, 17(2), 77-86.



Introduction

An effective drilling fluid is a key factor for a successful drilling operation. The fluid is pumped down the drilling column to the drill bit and returns through the annular space carrying cuttings to the surface, where they are removed by a separator so that the fluid can be recirculated in the borehole (Vryzas & Kelessidis, 2017). With wells reaching increasing depths, the challenge is growing to guarantee the borehole's stability during drilling in reactive formations, especially in the case of shale formations (Parizad, Ahahbazi & Tanha, 2018, Ismail, Rashid & Jaafar, 2014). In response to this challenge, it is necessary to formulate drilling fluids with suitable properties that can be maintained during the drilling work (Caenn, Darley & Gray, 2011; Ayala, Torres, Valencia & Loaiza, 2016). These fluids (also called drilling muds) are traditionally classified according to the base used to prepare them, generally water, oil or air (Medina, Martínez, León & Boada, 2013). Fluids can also be based on esters, ethers, polyalphaolefins, glycols, glycerins and glycosides, called synthetic fluids (Caenn & Chillingar, 1996).

In the majority of cases, oil-based fluids have good operational performance (Portilla, Suárez & Corzo, 2012). However, they have higher costs and potential pollution problems, so their use is limited by environmental legislation (Adesina, Anthony, Gbadegesin, Esehene & Oyakhire, 2012). Hence, environmental and cost questions explain the preference for water-based muds in wells with low, and sometimes even high, pressure (Fernandes & Young, 2010). These fluids, however, require additives to attain the needed rheological and filtration properties (Huarcaya, Tocas, Ruiz & Araque, 2019; Loaiza, Ayala, Torres & Ayala, 2018), since the invasion of the fluid in porous formations can damage and reduce the productivity of the reservoir, clog outflow pipes, and even cause the formation to collapse (Kosynkin et al., 2011; Sadeghalvaad & Sabbaghi, 2015; Silva & Lucas, 2018; Silva, Bertolino & Lucas, 2019; Guerrero, Montes, Oliveira, Cristina, Campos & Lucas, 2018).

Polymers are widely used in petroleum industry for many purposes (Lucas, Ferreira & Khalil, 2015; Figueira, Simão, Soares & Lucas, 2017). Polymeric additives can be used to optimize rheological properties in different types of drilling fluid. Additives that can be used in water-based muds to increase the low-shear-rate viscosities and gel strengths are, for example: xanthan gum (XG), carboxymethylcellulose (CMC), and partially-hydrolyzed polyacrylamide (PHPA).

The influence of the polymer/ surfactant system on reducing filter loss from aqueous aphron based drilling fluids is also known. Aphrons are a dispersion of gas microbubbles that are resistant and stable, resisting coalescence in larger bubbles. Some polymers that are used in the formulation of aphrons are: XG, PHPA, poly(ethylene oxide) (PEO) and poly(propylene oxide) (PPO) (Caenn & Chillingar, 1996; Lucas et al., 2009). Hydrosoluble polymers, including natural and modified ones, are among the additives used to affect the drilling fluid's viscosity. Their correct choice allows developing formulations with the properties necessary for the particular formation conditions (Garcia-Ochoa, Santos, Casas & Gómez, 2000; Pérez, Siquier, Ramírez, Muller & Sáez, 2004; Jiménez, Hernández, Delegido & Casanovas, 2007). Therefore, in light of the challenges of using water-based drilling fluids, including economic considerations, we prepared fluid formulations containing low concentrations of additives, aiming to find an inexpensive formulation that still has rheological and filtration parameters compatible with the API standards, to meet the typical operational needs in the oil and gas industry today (Ayala, Benítez & Valencia, 2017; Campana & Tapia, 2017).

Experimental

Materials

The following materials were used in this work: (i) xanthan gum (XG) (Newpark Drilling Fluids, Texas), used as viscosifier; hydroxypropyl starch (HPS) (Newpark Drilling Fluids, Texas), used as filtrate reducer; magnesium oxide (MgO) (Vetec, Rio de Janeiro), employed to control pH; potassium chloride (KCl) (Vetec, Rio de Janeiro) and the commercial product (Newpark Drilling Fluids, Texas), used to inhibit clay swelling; calcite (Vetec, Rio de Janeiro), used as a thickener; a commercial antifoam agent (Newpark Drilling Fluids, Texas); a commercial bactericide (Newpark Drilling Fluids, Texas); and deionized distilled water.

Preparing the fluids

The products were added during preparation of the fluids, under slow stirring with a mixing interval of 10 minutes for solid materials and 5 minutes for liquids. After addition of the products, the mixing speed was set to medium (Hamilton Beach blender).

Just after preparation, the rheology of the fluid was analyzed (Fann viscometer) before aging (before hot rolling – BHR). The formulations were then aged in a

rotating oven (roll over) for 16 hours at 49 °C. Then they were again submitted to rheology testing, i.e., after hot rolling (AHR), as well as filtration testing (API filter press). The formulations are identified in Tables 1 and 2. Table 1 presents the fixed concentrations of the components used in all the formulations, while Table 2 lists the quantities of the variable components (XG, HPS and KCl) in each formulation. The concentrations of the fixed polymers in formulations LA and LB (1.0 g and 1.5 g of HPA and XG, respectively) were chosen in light of the intrinsic economic factor of optimal formulations (Petrobras, Private Communication). KCl can reduce the viscosity (Moreira, 2007), which can cause an increased volume of filtrate. For this reason, in the LC formulations it was chosen to work at a concentration of 1.5 g of HPS.

Table 1. Components with fixed composition in the fluids.

Components of the fluid	Content
Water	350.0 mL
MgO	1.0 g
Commercial swelling inhibitor	6.0 g
Calcite	15.0 g
Bactericidal	5.0 drops
Antifoaming	5.0 drops

Table 2. Concentrations of the variables in different formulations.

Fluid components (g)	Fluid A			
	LA1	LA2	LA3	LA4
XG	0.5	1.0	1.5	2.0
HPS	1.0	1.0	1.0	1.0
KCl	16.0	16.0	16.0	16.0
	Fluid B			
	LB1	LB2	LB3	LB4
XG	1.5	1.5	1.5	1.5
HPS	1.0	1.5	2.0	2.5
KCl	16.0	16.0	16.0	16.0
	Fluid C			
	LC1	LC2	LC3	LC4
XG	1.5	1.5	1.5	1.5
HPS	1.5	1.5	1.5	1.5
KCl	0.0	8.0	16.0	24.0

Rheological analysis

Before and after aging (BHR and AHR), the fluids were analyzed with a Fann model 35A viscometer, using the R1 B1 combination, i.e., external cylinder radius of 1.8415 cm and internal radius of 1.7245 cm, and F1 torsion spring, i.e., a spring constant value of 1 (Machado, 2002). In this instrument, six deflection angles (torque) were read, with shear rates

varying from 5.1 to 1022 s⁻¹. The analytic procedure was based on API Spec 13A (1993). The instrument was operated at an initial speed of 600 rpm, and after stabilization of the pointer, readings were taken at 300, 200, 100, 6 and 3 rpm. The values obtained from these readings are respectively denominated Φ_{600} , Φ_{300} , Φ_{200} , Φ_{100} , Φ_6 and Φ_3 . From the deflection angles (ϕ), it was possible to determine the apparent (μ_a) and plastic viscosities (μ_p), as well as the yield point (γ_p), according to the same standard, obtained by the respective Equations 1, 2 and 3:

$$\mu_a = \frac{\Phi_{600}}{2} \text{ (cp)} \quad (1)$$

$$\mu_p = \Phi_{600} - \Phi_{300} \text{ (cp)} \quad (2)$$

$$\gamma_p = \Phi_{300} - \mu_p \text{ (N/m}^2\text{)} \quad (3)$$

The initial gel (G_i) and final gel (G_f) strength values were also obtained for the purpose of identifying the fluids' thixotropy degree. To obtain G_i , the viscometer was kept at 600 rpm during 1 minute and then was stopped for 10 seconds. After this interval, it was turned on again at 3 rpm to record the largest deflection on the indicator. The G_f value was determined similarly, with only the resting time different, which was 10 minutes rather than 10 seconds before reading the greatest deflection at 3 rpm. The gel force, according to the API standard followed, was determined by Equation (4).

$$F_g = G_f - G_i \text{ (lbf/100ft}^2\text{)} \quad (4)$$

According to Machado (2002), the analysis of the rheological behavior of the fluid through the deflection angles read on a rotational viscometer can be done by transforming rotations into shear stresses (τ) and shear rates ($\dot{\gamma}$) according to Equations (5), (6) and (7).

$$\tau = 0.51 \cdot \Phi \text{ (Pa)} \quad (5)$$

$$\tau = 1.067 \cdot \Phi \text{ (lbf/100ft}^2\text{)} \quad (6)$$

$$\dot{\gamma} = 1.703 \cdot N \text{ (s}^{-1}\text{)} \quad (7)$$

where ϕ is the deflection angle, and N is the speed in rpm.

After performing the mathematical calculations, flow curves we plotted (shear stress x shear rate) of the fluids.

The flow index (n) and consistency index (K) were determined considering the power model for fluids (Machado, 2002). To linearize the flow curve, the

experimental data were log-transformed, i.e., $\text{Log } \Phi \times \text{Log } N$. The flow or behavior index (n), dimensionless, and the consistency index (K), for the Fann 35A viscometer, configured in R1-B1 combination, F-1 spring, in $\text{lb}\cdot\text{s}^n/100\text{ft}^2$, were obtained, respectively, by Equations (8) and (9).

$$n = \frac{\log \Phi_2 - \log \Phi_1}{\log N_2 - \log N_1} \tag{8}$$

$$K_v = \frac{1.067 \cdot \Phi}{(1.703 \cdot N)^n} \tag{9}$$

Fluid aging test

This was accomplished by placing cells containing fluid samples in a Fann model 704Es roller oven for 16 hours at a temperature of 49 °C. Then the rheological properties of the fluids could be compared before and after aging. Based on the importance of the aging effect of mud at high temperatures, the objective of this test was to simulate the aging that would occur at typical well temperature during circulation.

Filtration test

This test was performed with an API LPLT (low pressure, low temperature) filter press, according to the conditions indicated in the API standard (Lomba, 2010). Pressure of 100 psi and permeability of 7.1 pol^2 were used, to simulate the pressure and permeability conditions within a well. This test was performed after the aging of the fluid.

Results and discussion

The results obtained will be referenced to the values accepted as optimal for the properties of the fluids, namely: apparent viscosity (μ_a) ≥ 15.0 cP; plastic viscosity (μ_p) $\geq 4,0$ cP; yield point (γ_p) $\leq 15x$ μ_p (N/m^2); filtrate volume (v_f) ≤ 14 mL (high yield) or 16 mL (medium yield); gel strengths - G_i (initial gel) of 3 to 12 $\text{lb}/100\text{ft}^2$ and G_f (final gel) of 8 to 20 $\text{lb}/100\text{ft}^2$ (API SPEC 13A, 1993).

Tables 3, 4 and 5 present the deflection angles, parameters, and filtrate volume values obtained, respectively, for fluid formulations A, B and C, before and after aged by hot-rolling. The bolded values are within the limits established by the standard. For the LA formulations (Table 3), an increase in the concentration of xanthan gum led to a rise of viscosity, revealing the efficiency of using the polymer as a viscosifier, since its rheological

properties allow the formation, at low concentrations, of viscous solutions and hydrosoluble gels (Luvielmo & Scamparini, 2009).

Fluid LA3 presented the best results. Formulation LA4 could not be selected because the initial gel strength values exceeded the limit established in the API standard (Spec 13A, 1993). During the fluid circulation in the well or during a maneuver (step in which the circulation of the fluid stops for a few moments), the high temperature can contribute to the degradation of the additives present in the fluid composition. Thus, knowledge of the unperturbed gel strength is very important, because it allows determining the pressure necessary for the mud to return to circulation (Caenn, Darley & Gray, 2011). Very high gel strength values are undesirable because when drilling starts again after a stop, high viscosity would require a huge mechanical force to cause the fluid to circulate again. On the other hand, gel strength values far below those stipulated by the API standard can cause clogging of the well due to the weak sustentation of the cuttings by the gel (Barros, Lachter & Nascimento, 2007).

Table 3. Properties of LA formulations, before (BHR) and after (AHR) hot rolling

	LA1		LA2		LA3		LA4	
	BHR	AHR	BHR	AHR	BHR	AHR	BHR	AHR
(rpm)	12	12	22	22	32	34	44	45
(rpm)	9	9	17	17	26	27	35	35
(rpm)	8	8	14	15	22	23	31	31
(rpm)	5	5	11	12	19	19	26	26
(rpm)	2	2	6	6	11	11	16	17
(rpm)	2	3	5	5	10	10	15	15
($\text{lb}/100\text{ft}^2$)	3	3	6	5	10	10	15	15
($\text{lb}/100\text{ft}^2$)	2	2	6	5	11	11	16	16
v_f (mL)	9.0		8.0		6.5		5.5	
μ_a (cp)	6.0	6.0	11.0	11.0	16.0	17.0	22.0	22.5
μ_p (cp)	3.0	3.0	5.0	5.0	6.0	7.0	9.0	10
γ_p (N/m^2)	2.87	2.87	5.75	5.75	9.58	9.58	12.45	11.70
n	0.33	0.24	0.27	0.27	0.22	0.23	0.20	0.18
K ($\text{N}\cdot\text{s}^n/\text{m}^2$)	0.60	1.04	1.65	1.65	3.37	3.30	5.13	5.66

The graph in Figure 1 represents the relation of the yield point and plastic viscosity with the XG concentration in the formulation (aged after hot rolling). The concentration is expressed as a percentage of the mass of the polymer by volume of water. It can be seen that the plastic viscosity and yield point have well-defined behavior, directly proportional to the rise of polymer concentration. The electrochemical interaction between

the solids in the fluid contribute to increase the yield point (Diaz, Vendruscolo & Vendruscolo, 2004; Albuquerque, Fagundes, Fagundes, 2017), and despite the increase, the plastic viscosity value is low in relation to the yield point and should be adjusted to prevent operational problems, such as drill pipe lock-up.

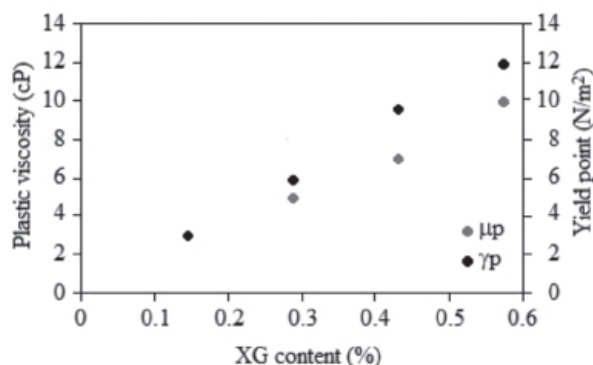


Figure 1. Influence of XG concentration (mass percent of polymer related to water volume) on the plastic viscosity (AHR) and the yield point (AHR) of the LA formulations.

The graph in Figure 2 presents the flow curves of formulation LA3 before and after aged by hot rolling. Both curves reflect pseudoplastic behavior, corroborating the value of the behavior index ($0 < n < 1$) presented in Table 3. During circulation, the fluid's constituents can degrade (Caenn, Darley & Gray, 2011). In the case of formulation LA3, the xanthan gum showed stability under shear and in the temperature range applied in the aged by hot rolling test, since the small variation between the BHR and AHR curves was within the error interval of the analysis. This was confirmed by regression statistical analysis, carried out with the mathematical tool generated by the software adjusted with 95% confidence. According to Freitas (2002), the stability promoted by the presence of a polymer can be explained by the three-dimensional network formed by the associations of its chains. This stability depends on the concentration, and is greater at higher concentrations (Pettitt, 1982).

Table 4 reports the results obtained from varying the concentration of the polymer hydroxypropyl starch (HPS) (Table 2). It can be seen that except for LB4, all the fluids had values within the limits of the API standard (Spec 13A, 1993). However, formulation LB3 presented the best results. The importance of studying the influence of varying the concentration of HPS is due to its ability to absorb a large quantity of water and to act as an efficient filtrate reducer. The value of 4.4 mL

found, besides being in conformity with the standard, is in line with the determination described by Almeida and Silva (2010) for reactive formations, by presenting a volume lower than 5 mL.

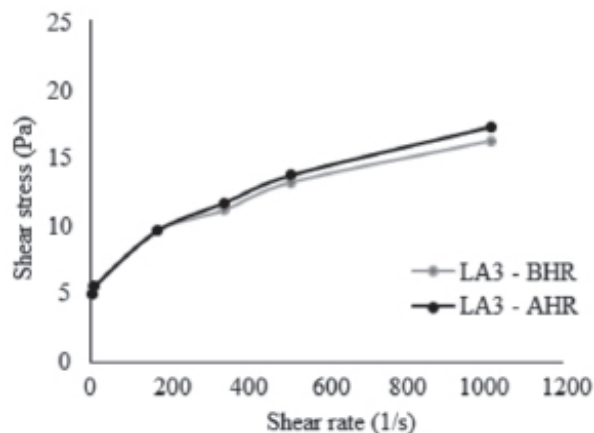


Figure 2. Shear stress versus shear rate of the fluid LA3 before (BHR) and after (AHR) aging

The graph in Figure 3 describe the relation of the yield point and plastic viscosity with the HPS concentration in the formulation (fluid after aging). The concentration is expressed as percentage of the mass of polymer per volume of water. It can be seen that up to a polymer concentration of approximately 0.57% (corresponding to fluid formulation LB3), the plastic viscosity increased, due to the greater friction because of the increased number of particles, and the yield point increased with alteration of the force between the particles (electrochemical reaction between the solids in the fluid) (Diaz, Vendruscolo & Vendruscolo, 2004; Albuquerque, Fagundes, Fagundes, 2017).

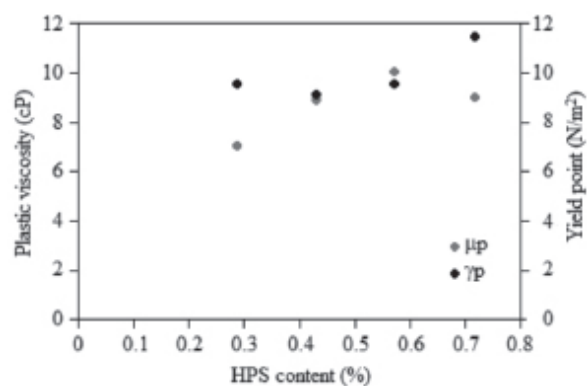


Figure 3. Influence of HPS concentration (mass percent of polymer related to water volume) on the plastic viscosity (AHR) and the yield point (AHR) of the LB formulations

Table 4. Properties of LB formulations, before (BHR) and after (AHR) hot rolling

	LB1		LB2		LB3		LB4	
	BHR	AHR	BHR	AHR	BHR	AHR	BHR	AHR
(rpm)	32	34	35	37	37	40	40	42
(rpm)	26	27	27	28	28	30	31	33
(rpm)	22	23	24	25	24	26	26	29
(rpm)	19	19	20	20	20	21	21	23
(rpm)	11	11	11	11	12	12	12	13
(rpm)	10	10	10	10	11	11	11	12
(lbf/100ft ²)	10	10	10	11	11	12	11	13
(lbf/100ft ²)	11	11	11	11	12	12	12	13
v _f (mL)	6.5		6.0		4.4		3.8	
μ _a (cp)	16.0	17.0	17.5	18.5	18.5	20.0	20.0	21
μ _p (cp)	6.0	7.0	8.0	9.0	9.0	10.0	9.0	9.0
γ _p (N/m ²)	9.58	9.58	9.10	9.10	9.10	9.58	10.53	11.49
n	0.22	0.23	0.23	0.24	0.22	0.23	0.24	0.24
K (N.s ⁿ /m ²)	3.37	3.30	3.30	3.23	3.71	3.56	3.49	3.82

For formulation LB3, the distance obtained between the plastic viscosity and yield point values are adequate to start the laminar flow in the suspension without subjecting the operation to a high risk of tooling becoming trapped. An increase in apparent viscosity is also shown, where the value found in fluid LB3 favors well cleaning without overloading the mud pump. The apparent viscosity value influences the filtrate volume, as indicated by relation between reduction of filtrate volume and increase of apparent viscosity.

According to the literature (Whistler & Paschall, 1965), the presence of hydroxypropyl groups in the starch reduces its gelling temperature, i.e., the starch molecules, when submitted to continuous heating in the presence of water, tend to vibrate more intensely at lower temperatures, breaking the intermolecular hydrogen bridges and allowing water to penetrate the micelles (crystalline zones), which results in total loss of those zones and facilitates swelling of the starch granules, increasing the viscosity of the suspension, and at the extreme forming a viscous paste. The swollen granules can be broken and disintegrated by the shear force or agitation of the paste, resulting in lower viscosity. The pseudoplastic behavior of the system can be seen in the graph of Figure 4, which presents the flow curves of formulation LB3 before and after aging. The properties of the fluid remained relatively stable with aging, as demonstrated by the small variation between the curves, similar to the results for fluid LA3 (Figure 2).

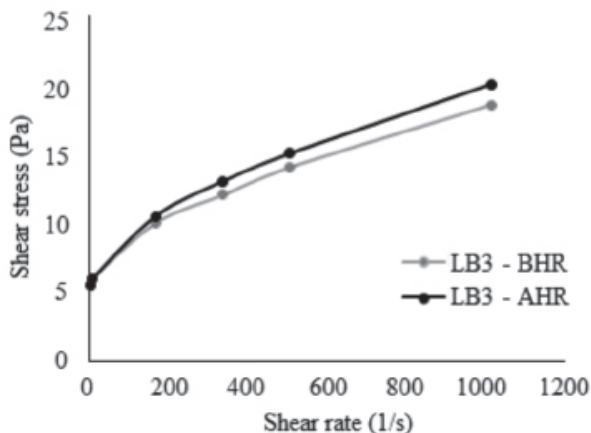


Figure 4. Shear stress versus shear rate of the fluid LB3 before (BHR) and after (AHR) aging

Table 5 gives the values attained by varying the concentration of salt (KCl) (Table 2). The increase of salt concentration caused a reduction of viscosity and increase of filtrate volume. According to Moreira (2007), in an investigation of the addition of salts in XG solutions, the effects on viscosity present contradictory results, with the possibility of increase or decrease of the viscosity of these solutions in the presence of salts. The explanation for this is based on the fact that XG, as a polyelectrolyte, presents a highly expanded conformation under low ionic force and is transformed into the randomly coiled type (more compact conformation) due to the shielding of the polymer charges by the salt ions at high concentrations, reducing the hydrodynamic volume and consequently the viscosity (Morris, 1984; Diaz, Vendruscolo & Vendruscolo, 2004).

Except for formulation LC1, whose *Gi* value was above the limit, all the others presented results within the limits established by the standard. However, formulation LC2 can be considered the most suitable for having the lowest filtrate value (5.5 mL). As already mentioned, this value is near that adequate for reactive rock formations (Almeida & Silva, 2010).

The graph in Figure 5 depicts the linear decrease of the yield point and a behavior that can be considered as having constant plastic viscosity (focusing the analysis on the AHR simulation test). The plastic viscosity behavior can be explained by the way the solids in the fluid interact as the concentration of KCl rises. According to Shiroma (2012), the plastic viscosity indicates the resistance of the fluid to its own movement. Solutions of XG can remain stable in the presence of salts due to the maintenance of some degree of order obtained

with the heating (Sutherland, 2001). The reduction of the yield point can be explained by the attenuation of the electrochemical forces between the fluid's particles.

The graph in Figure 6 contains the flow curves before and after aging of fluid LC2, indicating pseudoplastic behavior, corroborating the flow index value ($0 < n < 1$) reported in Table 5. Besides this, the system remained stable after aging, since the variation between the BHR and AHR curves can be considered negligible, as was seen for the curves in Figures 2 and 4.

Table 5. Properties of LC formulations, before (BHR) and after (AHR) hot rolling

	LC1		LC2		LC3		LC4	
	BHR	AHR	BHR	AHR	BHR	AHR	BHR	AHR
(rpm)	41	37	36	36	35	37	32	34
(rpm)	31	29	26	28	27	28	25	26
(rpm)	28	25	24	25	24	25	22	22
(rpm)	24	21	19	20	20	20	18	18
(rpm)	14	12	11	11	11	11	10	10
(rpm)	13	10	10	10	10	10	9	9
(lbf/100ft ²)	13	11	10	10	10	11	10	10
(lbf/100ft ²)	14	12	12	11	11	11	11	10
v _f (mL)	4.4		5.5		6.0		6.5	
μ _s (cp)	20.5	18.5	18.0	18.0	17.5	18.5	26	17
μ _p (cp)	10	8.0	10	8.0	8.0	9.0	7.0	8.0
γ _p (N/m ²)	10.05	10.05	7.66	9.58	9.10	9.10	8.62	8.62
n	0.20	0.23	0.22	0.24	0.23	0.24	0.23	0.24
K (N.s ⁿ /m ²)	4.46	3.63	3.37	3.23	3.30	3.23	2.96	2.90

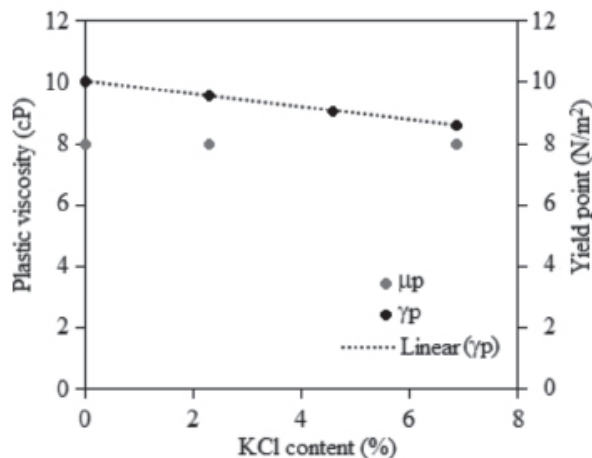


Figure 5. Influence of KCl concentration (mass percent of polymer related to water volume) on the plastic viscosity (AHR) and the yield point (AHR) of the LC formulations

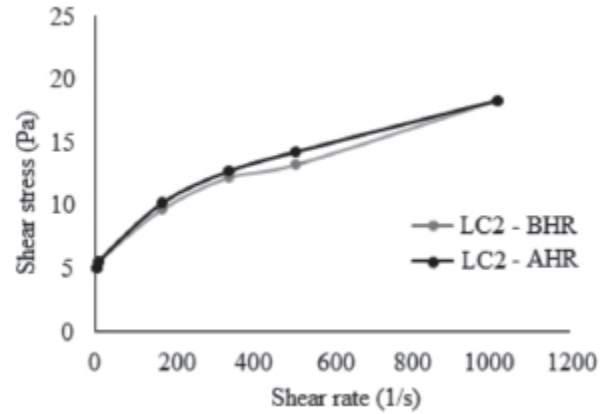


Figure 6. Shear stress versus shear rate of the fluid LC2 before (BHR) and after (AHR) aging.

The consistency index values (K) of formulations A, B and C will be discussed based on the graph presented in Figure 7. This consistency index indicates the relative degree of resistance of the fluid to flowing, so that higher values of K mean more viscous fluids. The objective is to find a consistency index that is sufficiently high to meet the need to keep the cuttings in suspension (Borges et al., 2009).

The graph in Figure 7 depicts the consistency index values in function of concentrations of XG, HPS and KCl. As these concentrations increased, the consistency indices presented, respectively, a considerable increase, a slight increase and a moderate decrease. KCl is an additive used to inhibit the swelling of reactive formations. This effect is due to the fact that the salt cations have diameters smaller than those of water and tend to remain between the clay layers, preventing hydration of the clay. Therefore, when dissolved in water, these cations separate and become available in the solution, where they are attracted by the negative surface charge of the clay, promoting control of its expansion by preventing an increase in the interplanar basal spacing of those formations in the presence of water (Lucena, Souto, Lira & Amorim, 2014). However, as already observed in Table 5, the presence of higher salt concentrations affects the compatibility of the other additives in the fluid, reducing the viscosity and increasing the filtrate volume. According to Almeida and Silva (2010), the presence of KCl can decrease the rheological modification effect, in turn reducing the polymer's solubility.

According to Oppermann, Ronald & Prud'homme (1992), the strategy of preparing hydrocolloid mixtures with good physico-mechanical properties is often advantageous, since it enables combining in

a single material two or more physico-mechanical properties desired for the particular application. This is reflected in the satisfactory behavior indicated in Figure 7, through manipulation of the concentrations of the hydrocolloid polymers.

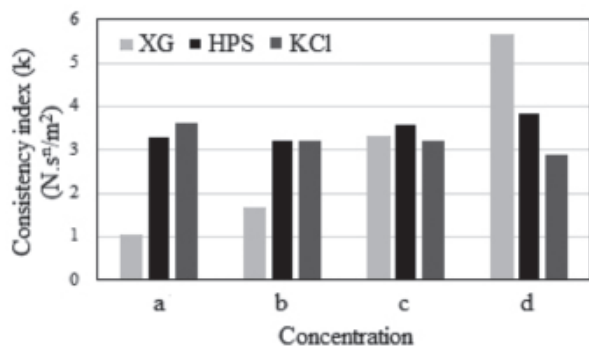


Figura 7. Consistency index (k) as a function of formulations compositions.

XG: a = 0.5 g, b = 1.0 g, c = 1.5 g, d = 2.0.
 HPS: a = 1.0 g, b = 1.5 g, c = 2.0 g, d = 2.5 g.
 KCl: a = 0.0 g, b = 8.0 g, c = 16.0 g, d = 24.0 g.

Conclusions

Three groups of formulations were evaluated, with variation of the concentrations of xanthan gum (XG), hydroxypropyl starch (HPS) and potassium chloride (KCl), respectively in formulations LA, LB and LC. The parameters determined were: initial gel strength (G_i), final gel strength (G_f), apparent viscosity (μ_a), plastic viscosity (μ_p), yield point (γ_p), filtrate volume (v_f), consistency index (K) and flow index (n).

The results for the LA formulations indicated that the increase in the concentration of XG led to values of G_f , μ_a and μ_p within the limits of the standard, although the values of G_i exceeded the limit required of a fluid with good performance. The ideal XG concentration was 0.43% m/v. Because of the high filtrate volume (greater than 5 mL), its use should be avoided in formations composed of reactive shale layers.

The analysis of the LB formulations indicated that the increase in the concentration of HPS reduced the filtrate volume, but increased G_i to values exceeding the limit established by the standard. The ideal concentration of HPS was found to be 0.57 %m/v, which led to a filtrate volume of 4.4 mL, reducing the risk of use in reactive formations and enabling an increase in the plastic viscosity value, necessary to prevent operational problems such as drill pipe lock-up.

With respect to the LC formulations, low KCl concentrations helped to reduce the filtrate volume, while high concentrations interfered in the functions of the other polymers included in the fluid. However, it is not interesting to reduce the concentration of this salt because it is inexpensive and also works to inhibit swelling. With an increased quantity of KCl, the filtrate volume can be kept in check by increasing the amount the filtrate reducing agent. Thus, the ideal KCl concentration is 4.57 %m/v.

Based on the results obtained and the testing method, formulation LB3 has the highest technical-economic feasibility for drilling operations, with concentrations of 0.43% m/v of the viscosifier polymer (XG), 0.57% m/v of the filtrate reduction polymer (HPS) and 4.57% m/v of the clay swelling inhibitor. For future work, it would be interesting to analyze the action of another salt, such as NaCl, on rheological properties based on the formulations presented. And also to study the behavior of the fluid in high pressure and high temperature conditions, using high temperature filter press (HPTP).

Acknowledgements

The authors thank FAPERJ (E-26/201.233/2014), CNPq (307193/2016-0) and CAPES for the financial support.

References

- Adesina, F., Anthony, G., Gbadegesin, A., Eseighene, O., Oyakhire, A. Environmental Impact Evaluation of a Safe Drilling Mud. Middle East Health, Safety, Security, and Environment Conference and Exhibition. Abu Dhabi, 2012
- Albuquerque, U. R., Fagundes, F. P., Fagundes, K. R. S. Influence of bivalente cations (Ca^{2+} e Mg^{2+}) in the rheological and filtration properties of aqueous drilling fluids. Revista Eletrônica de Petróleo e Gás (RUnPetro, UP), Rio Grande do Norte, 1, 9-15, 2017.
- Almeida, R. D. F., Silva, W. G. A. L. Avaliação de fluidos de perfuração de base aquosa contendo poliglicóis modificados. Escola Politécnica, Universidade Federal do Rio de Janeiro, Rio de Janeiro; 2010.
- API Specification 13A (Spec 13A) – American Petroleum Institute, Specification for Drilling Fluid Materials – Washington, 1993.
- Ayala, D., Benítez, A., & Valencia, R. (2017). Optimización de la Tasa de Penetración mediante el análisis de las vibraciones al perforar, caso de estudio Ecuador. *Revista Fuentes*, 15(1), 27-40.

6. Ayala, D., Torres, H., Valencia, R., & Loaiza, M. (2016). Impacto del Tiempo no Productivo en operaciones de perforación y análisis de los datos mediante la prueba de Chicuadrado. *Revista Fuentes*, 14(2), 5-18.
7. Barros, A.O., Lachter, E.R., & Nascimento, R.S.V. Estabelecimento de correlações estrutura propriedades de acetais para fluidos de perfuração, 4º PDPETRO, Campinas, SP, 2007.
8. Borges, D. et al. Comportamento Reológico de Xantana Produzida por *Xanthomonas arboricola* pv *pruni* para Aplicação em Fluido de Perfuração de Poços de Petróleo. *Polímeros: Ciência e Tecnologia*, 19, 2, 160-165, 2009.
9. Caenn, R., Chillingar, G. V. Drilling Fluids: State of the Art. *Journal of Petroleum Science and Engineering*, 14, 221-230, 1996.
10. Caenn, R, Darley, H. C. H., Gray, G. R. Composition and properties of drilling and completion fluids. 6 ed. Gulf Professional Publishing, 2011.
11. Campana, D. E. A., & Tapia, R. A. V. (2017). Evaluación cualitativa de la limpieza de hoyo en pozos de alta inclinación-alto desplazamiento en la Cuenca Oriente. *Revista Fuentes*, 15(2), 49-56.
12. Diaz, S., Vendruscolo, T., Vendruscolo, S. Reologia de Xantana: uma Revisão sobre a Influência de Eletrólitos na Viscosidade de Soluções Aquosas de Gomas Xantana. *Ciências Exatas e Tecnológicas*, 25, 15-28, 2004.
13. Fernandes, J. M., Young, S. Environmentally Responsible Water- Based Drilling Fluid for HTHP Applications. AADE Fluids Conference and Exhibition. Texas, p. 6-7, 2010.
14. Figueira, J. N., Simão, R. A., Soares, B. G., Lucas, E. F. The influence of chemicals on asphaltene precipitation: a comparison between atomic force microscopy and near infrared techniques. *Fuentes: El Reventón Energético*, 15, 7-17, 2017.
15. Freitas, I. C. Estudo das interações entre biopolímeros e polpas de frutas tropicais em cisalhamento estacionário e oscilatório. Universidade de Campinas: Campinas, 2002.
16. Garcia-ochoa, F., Santos, V. E., Casa, A., Gómez, E. Xanthan gum: production, recovery and properties. *Biotechnology Advances*, New York, 18, 549-579, 2000.
17. Guerrero-Martin, C. A., Montes-Páez, E., de Oliveira, K., Cristina, M., Campos, J., & Lucas, E. F. (2018, June). Calculating Asphaltene Precipitation Onset Pressure by Using Cardanol as Precipitation Inhibitor: A Strategy to Increment the Oil Well Production. In *SPE Trinidad and Tobago Section Energy Resources Conference*. Society of Petroleum Engineers.
18. Huarcaya, J. C. S., Tocas, W. E. C., Ruiz, D. O., & Araque, A. D. P. B. (2019). Evaluación del uso de almidón de papa como aditivo para lodos de perforación. *Revista Fuentes*, 17(1), 19-28.
19. Ismail, A.R., Rashid, N.M., Jaafar, M.Z. Effect of nanomaterial on the rheology of drilling fluids. *Journal of applied sciences*, 14, 1192-1197, 2014.
20. Jiménez, M. J., Hernández, M. J.; Delegido, J., Casanovas, A. Flow and thixotropy of non-contaminating oil drilling fluids formulated with bentonite and sodium carboxymethyl cellulose. *Journal of Petroleum Science and Engineering*, 56, 294-302, 2007.
21. Kosynkin, D.V., Ceriotti, G., Wilson, K., Lomenda, J., Scorsone, J.T.; Patel, A.D.; Friedheim, J.E.; Tour, J.M. Graphene Oxide as a High-Performance Fluid-Loss-Control Additive in Water-Based Drilling Fluids. *ACS Applied Materials e Interfaces*. U.S., 4, 222-227, 2012.
22. Loaiza, M., Ayala, D., Torres, H., & Ayala, S. (2018). Tiempo no productivo en pozos de dos secciones, caso de estudio Ecuador. *Fuentes: El reventón energético*, 16(1), 7-17.
23. Lomba, R. Fundamentos de filtração e controle de filtrado de fluidos de perfuração. Rio de Janeiro, 2010.
24. Lucas, E. F., Mansur, C. R. E., Spinelli, L., Queirós, Y. G. C. Polymer science applied to petroleum production. *Pure and Applied Chemistry*. Rio de Janeiro, 81, 473-494, 2009.
25. Lucas, E. F., Ferreira, L. S., Khalil, C. N. Polymers Applications in Petroleum Production, in: *Encyclopedia of Polymer Science and Technology*, Mark, H. F., ed., John Wiley & Sons, New York, 2015.
26. Lucena, D. V., Souto, C. M. R. A., Lira, H. L., Amorim, L. V. Influência de sais de potássio como inibidores de inchamento de folhelhos no desempenho de fluidos de perfuração poliméricos. *Tecnol. Metal. Mater. Miner. São Paulo*, 11, 355-362, 2014
27. Luvielmo, M.; Scamparini, R.P. Goma Xantana: produção, recuperação, propriedades e aplicação. *Estudos tecnológicos*, 5, 50-67, 2009.
28. Machado, J.C.V. Reologia e escoamento de fluidos. Rio de Janeiro, Editora Interciência, 2002.
29. Medina, C. A. C., Martínez, J. J. S., León, E. A., & Boada, W. M. (2013). Análisis reológico

- para predecir y mejorar el comportamiento hidráulico durante la perforación de un pozo. *Revista Fuentes*, 11(1).
30. Moreira, G. P. et al. Estudo comparativo entre novo emulsificante e produtos comerciais na estabilidade de fluidos de perfuração à base de éster – 4º PDPETRO – Campinas – SP, 2007.
 31. Morris, E. R. Rheology of hydrocolloids. In: Phillips, G.O.; Wedlock, D.J.; Willians, P.A. Gums and stabilisers for the food industry. Oxford: Pergamon Press, 1984. 57-78.
 32. Oppermann, W., Ronald, S. H. E Prud'homme, R. K., Polyelectrolyte Gelspreparation and application, Ed. ACS, Washigton, DC, cap 10, 150, 1992.
 33. Parizad, A., Shahbazi, K.; Tanha, A. Enhancement of polymeric water-based drilling fluid properties using nanoparticles. *Journal of Petroleum Science and Engineering*. Iran, v.170, p. 813-828, 2018.
 34. Pérez, R.M., Siquier, S., Ramírez, N, Muller, R.A.J.; Sáez, A.E. Non-Newtonian annular vertical flow of sand suspensions in aqueous solutions of guar gum. *Journal Petroleum Science and Engineering*, 44, 317-331, 2004.
 35. Pettitt, D. J. Xanthan gum. *Food Hydrocolloids*, 1, 127-149, 1982
 36. Portilla, H. E., Suárez, D. F., & Corzo, R. (2012). Metodología para la optimización de parámetros de perforación a partir de propiedades geomecánicas. *Revista Fuentes*, 10(2).
 37. Sadeghalvaad, M., Sabagi, S. The effect of the TiO₂/polyacrylamide nanocomposite on water-based drilling fluid properties. *Powder Technology*. Iran, 272, 113–119, 2015
 38. Shiroma, P. h. Estudo do comportamento reológico de suspensão aquosa de bentonita e CMC: influência da concentração do NaCl. Ed. Versão São Paulo, 130, 2012.
 39. Silva, I. G. M., Lucas, E. F. Rheological properties of xanthan gum, hydroxypropyl starch, cashew gum and their binary mixtures in aqueous solutions. *Macromolecular Symposia*, 380, 1800070 (1-9), 2018.
 40. Silva, I. G. M., Bertolino, L. C., Lucas, E. F. Correlation between clay type and performance of swelling inhibitors based on polyetherdiamine in aqueous fluids. *Journal of Applied of Polymer Science*, 136, 47661, 2019.
 41. Vryzas, Z., Kelessidis, V. Nano-Based Drilling Fluids: A Review. *Energies*. Qatar, 540, 10, 1-34, 2017.
 42. Whistler, R. L., Paschall, E. F. *Starch: Chemistry and Technology*, Academic Press, New York, 1965.

Recepción: 10 de abril de 2019
Aceptación: 16 de diciembre de 2019